Plasmonics (2018) 13:305–313
DOI 10.1007/s11468-017-0515-3

Thermal Manipulation of Gold Nanocomposites for Microfluidic Platform Optimization

Michael Fanous[1] · **Simona Badilescu**[1] · **Muthukumaran Packirisamy**[1]

Received: 21 July 2016 / Accepted: 3 January 2017 / Published online: 25 January 2017

Abstract Surface gold–polymer nanocomposites are prepared by using the thermal convection method for the deposition of gold colloids onto the surface of four polymer films: poly(-vinyl alcohol) (PVA), SU-82, poly(styrene) (PS), and poly(dimethyl siloxane) (PDMS). In order to increase the plasmonic sensitivity of the platforms, the nanocomposites are, subsequently, subjected to an incremental heating in the range of 80–200 °C. As a consequence, small aggregates are formed and uniformly dispersed on the surface of the film. In addition, because of the softening of the polymer, a small fraction of nanoparticles "sinks" into the surface layer. Because of the different thermal properties of the polymers and the interactions between the nanoparticles and the polymer chains, the final configuration of the thermally "manipulated" nanocomposites will not be the same. It is found that, among the polymers studied in this work, PVA and SU-82 show the largest shift of the Au localized surface plasmon resonance (LSPR) band upon the incremental heating as well as the highest plasmonic sensitivity. It is thought that the thermal manipulation may be a useful method for increasing the plasmonic sensitivity of a platform. The results of this work will be helpful in selecting the best material for microfluidic sensing experiments.

Keywords Gold LSPR · Polymer nanocomposite · Thermal manipulations · Dark field hyperspectral imaging

✉ Muthukumaran Packirisamy
ammic123@gmail.com

[1] Optical-Bio Microsystems Laboratory, Mechanical and Industrial Engineering Department, Concordia University, Montreal, Canada

Introduction

Gold nanoparticles have been utilized throughout history to exploit their vermilion color in glass [1, 2]. Their remarkably low refractive index has also proven a very desirable property for applications such as biochemical sensing and detection. As well, gold nanoparticles exhibit increased absorption and light scattering when their dimensions are less than the wavelength of incident light [3].

The functional usages of these materials alone and in association with polymers largely involve their transparency in the Vis spectral range and, most importantly, surface plasmon resonance and, in some cases, optical nonlinearity [4]. The combination of polymer and Au nanoparticles entails numerous areas of implementation, including electron and energy storage and catalysis. In terms of medical applications, gold nanoparticles have high biocompatibility and can be paired to a multitude of biomolecular ligands, antibodies, and other biological entities, making them constructive agents for sensing and therapeutic applications. Colloidal gold nanoparticles are increasingly effective imaging elements due to their lack of cytotoxicity in immunotargeting [5], as well as their high resistance to photobleaching or chemical disintegration [6]. They have been used successfully in cancer diagnosis and treatment, cancer cell imaging [7–9], and drug release [10]. The capacity of gold nanoparticles to efficiently transform absorbed light into heat can be tapped for medical purposes, such as the photothermal destruction of cancerous cells. Further, Loo et al. have achieved imaging, in unison with therapy, of breast cancers in vitro employing silica-gold nanoshells tethered to anti-Her2 antibodies [11].

The combination of polymers with metals results in a number of transitions in property. These changes are influenced by the size, shape, and distribution of particles. Enlarging the particle diameter, for example, leads to

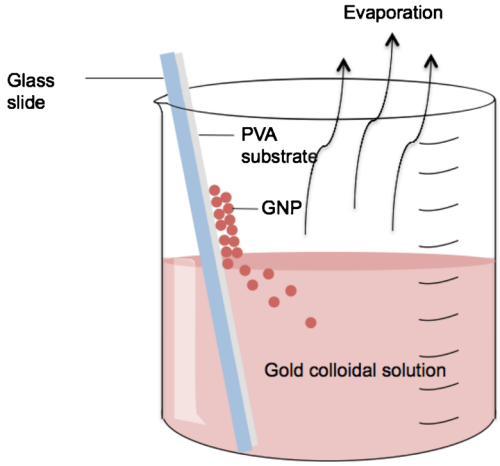

Fig. 1 Schematic of the convective assembly procedure of deposition of gold nanoparticles (MS Office)

absorption maximums of higher wavelengths [9]. Additionally, once the particles assemble, forming aggregates, their surface plasmons are coupled to produce extinction bands at longer wavelengths [12].

Another property of gold nanoparticles that must be accounted for is their high surface energy. Agglomeration of inorganic particles is promoted by their high surface energies, which generally exert up to 500–2000 mJ/m^2 in comparison with 20–50 mJ/m^2 for polymers [3]. This property, in combination with a heated polymer that undergoes softening, will lead to particles being submerged by the polymer to diminish their surface energies, resembling an "embedding" effect. The arrangement of these polymer-embedded particles induces various property changes. The degrees that the particles are lodged and their order, depths, and spacing of their immobilization are parameters that cause a specific dielectric environment, which in turn affect the electronic and optical responses of the hybrid material [13].

Nanocomposites can be fabricated in a number of different ways. Because of the low chemical potential of Au, ions can be easily reduced in the presence of even weak reducing agents. One method to achieve gold nanoparticles embedded in the surface of a polymer involves in situ reduction of $HAuCl_4$ inside a thin polymer film, leading to the formation of gold nanoparticles of various shapes [14]. We and other groups developed gold–polymer nanocomposites through in situ methods and built sensing platforms based on the gold localized surface plasmon resonance (LSPR) band [14]. Other techniques involve functionalizing a polymer (in this case poly(vinyl alcohol) (PVA)) with (3-mercaptopropyl)trimethoxysilane (MPTMS) producing a thiol functionality on its surface. Thereafter, gold particles are embedded on the surface of partially dried functionalized PVA, whereupon the gold particles are chemisorbed onto the thiol groups [9]. A polymer and precursor can also be first mixed in a common solvent and, immediately thereafter, the nanocomposite film is formed by evaporation of the solvent [13]. In another process to generate silver nanoparticles in a polymer, Porel et al. carried out an in situ fabrication, using an aqueous solution of silver nitrate and PVA for the fabrication of a free-standing film. In this case, PVA serves as both a reducing agent of the nanoparticles and as the host for uniform dispersion and suspension [15].

The effect of heating on a gold–polymer nanocomposite film has previously been investigated. For example, Liu showed that heating a composite at 90 °C caused the gold particles to become entirely enveloped by the polymer material (in this case poly(methyl methacrylate) (PMMA)). In this work, it was thought that the formation of the composite was facilitated at the glass transition temperature (Tg) of the gold–PMMA composite [10]. The new viscous state of the polymer surface induces a flow around the nanoparticle and adsorbs

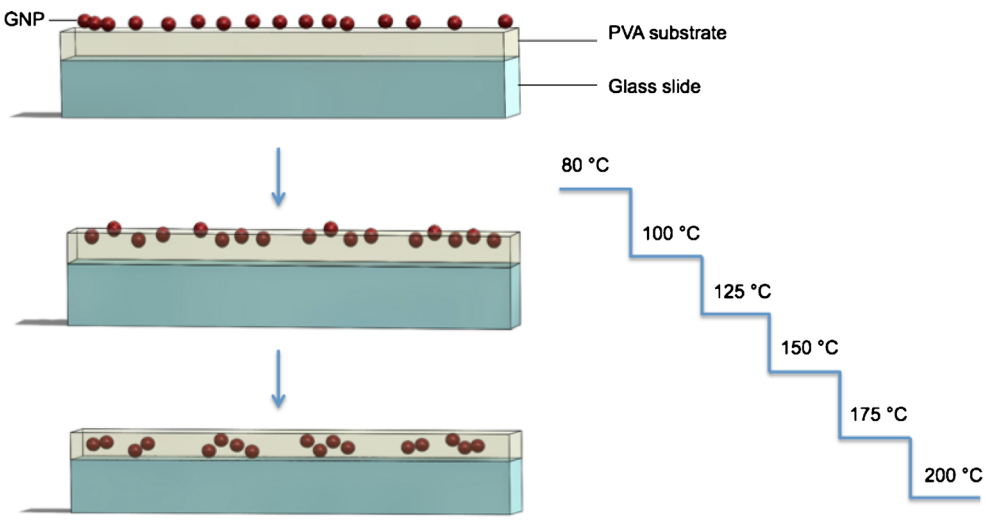

Fig. 2 Schematic depicting the gradual morphological changes through incremental heat treatment of AuNPs–polymer nanocomposites (SolidWorks)

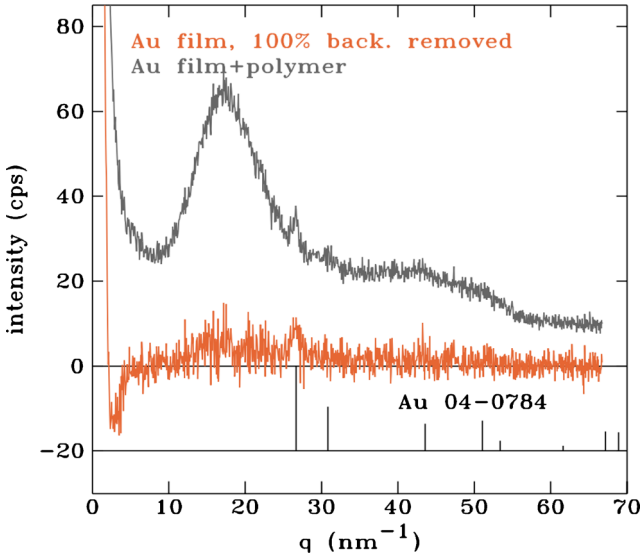

Fig. 3 X-ray diffraction (XRD) measurements on AuNPs without a polymer substrate (on glass slide) and a PVA sample with AuNPs heated

onto the nanoparticles' surface, decreasing their surface energy [16].

Generally, it has been confirmed experimentally that heating gold aggregates at 400–500 °C provoked a blueshift and a narrowing of the Au LSPR band, with a beneficial effect on sensing. However, to the best of our knowledge, the behavior of gold–polymer surface nanocomposites under incremental heat treatment at lower temperatures has *not* been reported. Our preliminary results have shown a large redshift of the Au LSPR band when some surface nanocomposites were heated incrementally and, to describe this technique, we coined the term "thermal manipulation."

Herein, we report a highly detailed analysis of thermal manipulation of Au particles embedded in polymers that vary from previous development and examination of this phenomenon in various respects. In this work, the nanocomposites are subjected to systematic heating that enables investigation of the material at different stages of heat treatment, both at the cross section and on the surface of the composite material. The convective method of evaporating a gold colloidal solution onto the polymer films is novel for this type of experiment and allows for the gradual evaluation of particle penetration from the surface to the bottom of the film. The sensitivity and other composite properties are measured for six different surface nanocomposites. The results obtained in this work will provide invaluable information for selecting the best materials for microfluidic sensing.

Experimental

Fabrication of the Gold–Polymer Nanocomposites

The polymers studied in this work are PMMA, poly(styrene) (PS), SU-82, poly(vinyl alcohol) (PVA), and poly(dimethyl siloxane) (PDMS). The solutions of the polymers were prepared by using a suitable solvent. For poly(styrene), a 5 % solution was prepared in anhydrous toluene. Poly(vinyl alcohol) was dissolved in water to a concentration of 5 %. SU-82 was purchased as a liquid, while PMMA (495 A11) was purchased as a solution. SU-82 is a type of negative photoresist that is epoxy-based.

PDMS was fabricated by first mixing a curing and base agent in a ratio of 1:10 in a small transparent container until the resulting mixture had a milky appearance. The mixture was then placed in a desiccator, and the vacuum was turned on and off for short elapses, in order to expel the air from the mixture. The solutions of the polymers were spin-coated on glass substrates and thereupon annealed at a temperature and duration that are specified according to their properties. The films were kept in the oven for 2 h at a temperature between 60 and 80 °C to remove the traces of solvent. Cyclic olefin copolymer was purchased in the form of a solid sheet.

A colloidal solution was used to deposit gold nanoparticles on the polymer films through a thermal convection method. This technique involves the transfer of gold nanoparticles from the colloidal solution onto the polymer film through evaporation and assembly. Spherical gold nanoparticles were produced according to Turkevich's method [14], employing

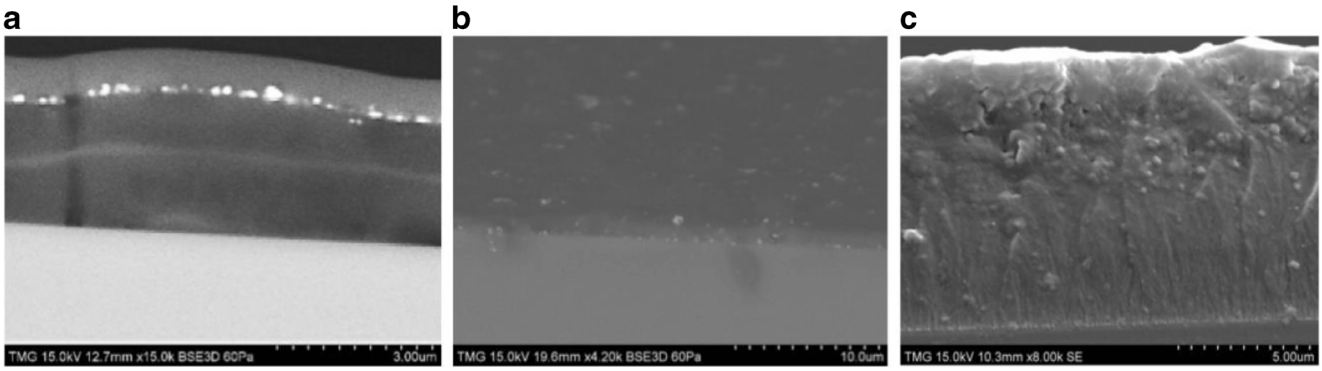

Fig. 4 SEM images of gold–polymer cross section. **a** AuNPs on PVA at room temperature. **b** Au-PVA nanocomposite heated at 175 °C. **c** SU-82 heated at 250 °C

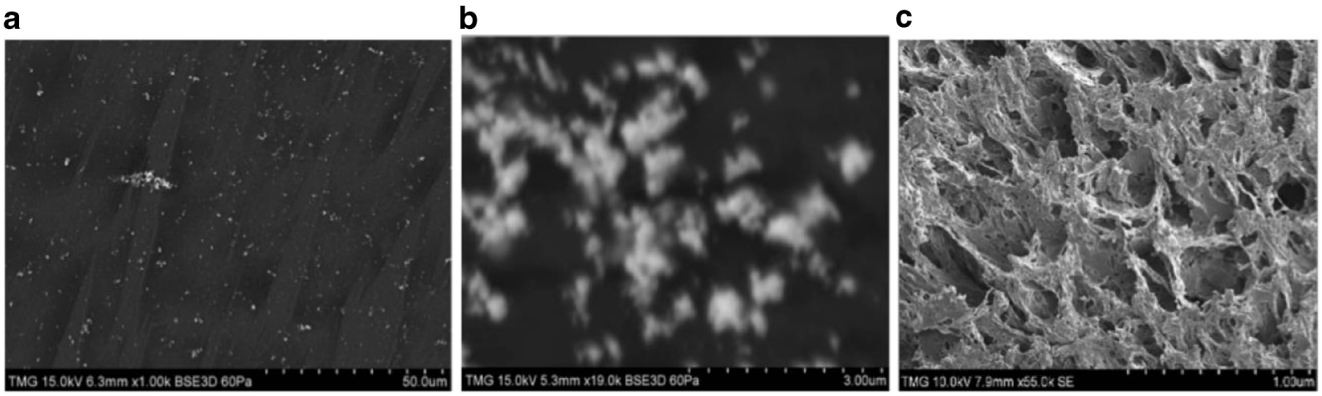

Fig. 5 SEM images of gold–polymer surfaces of **a**, **b** AuNPs on heated PVA and **c** PVA at room temperature

the reduction of chloroauric acid by sodium citrate. The solution was prepared from 1 mM of gold(III) chloride trihydrate dissolved in 90 ml of water, which was subsequently boiled. Fifteen milliliters of a sodium citrate solution (2 %) was added, and the solution was heated until the color of the solution became red-purple. After that, the solution was further boiled for 15 min and then left to cool to room temperature.

The gold colloidal solution was evaporated onto the slanted (inclined, slightly angled) polymer samples in a beaker and the gold nanoparticles were self-assembled through a convective assembly process, as shown in Fig. 1. Once immersed in the solution, the slides were kept in the oven until the whole amount of gold was transferred to the substrate, typically a duration of 2 days.

The polymer films, having the gold particles on their surface, were heated gradually, starting from 80 °C and increasing the temperature in increments of 25 °C for durations of 10 min each. This approach enables progressive measurements of the samples as they are being heated. The first temperature of heating is 80 °C and, after 10 min, the slides are taken out of the oven and left to cool to room temperature, before recording the spectrum. They are subsequently placed in the oven at 100 °C for another 10 min. This process is repeated at temperature increments of 25 °C, and the cycle is continued until right before the polymer's decomposition. A comparative slide of PVA, heated directly at 200 °C for 30 min, was also used for comparison. This process, and the possible resulting effects, is depicted in Figs. 2 and 3. For measurements involving examinations of the cross section of the samples, a diamond cutter was employed to incise across the deposited ends of the slides.

A method used to quantify the sensitivities of the nanocomposite platforms involved immersing the slide in solvents of distinct refractive indices, such as ethanol and toluene, and measuring the LSPR shift between them.

Methods

The methods employed to examine the interaction between the gold nanoparticles and the polymers are UV–visible spectroscopy (PerkinElmer's LAMBDA 650), scanning electron microscopy (S-2499n model from HITACHI and Oxford Instruments), atomic force microscopy (3100 AFM model), Raman spectroscopy using a 795-nm laser, Fourier transform infrared spectroscopy (FTIR), and hyperspectral microscopy (CytoViva).

UV–visible spectroscopy was used to assess the position of the localized surface plasmon resonance peaks at the varying temperatures. SEM and AFM were utilized both to image the surface of the slides, to discern the distribution of particles,

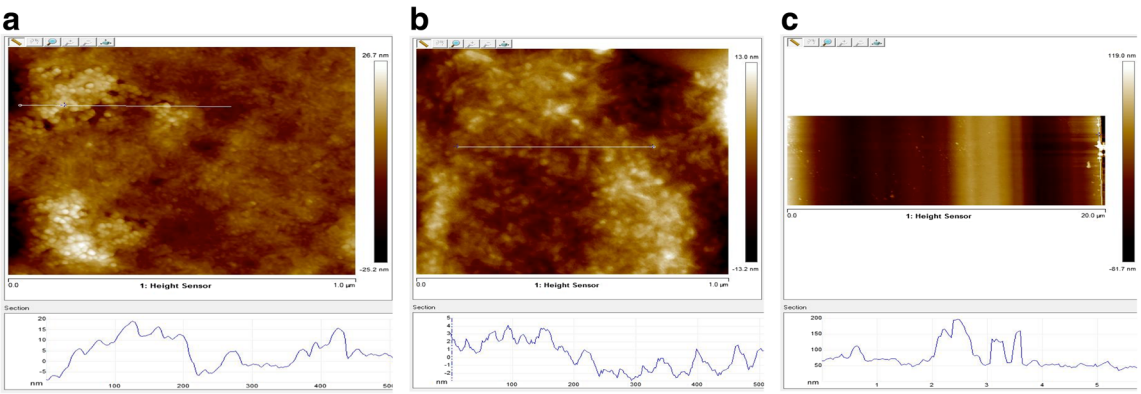

Fig. 6 **a** AFM image of non-heated Au-PVA. **b** AFM image of Au-PVA heated at 225 °C. **c** Cross-section image of the heated PVA

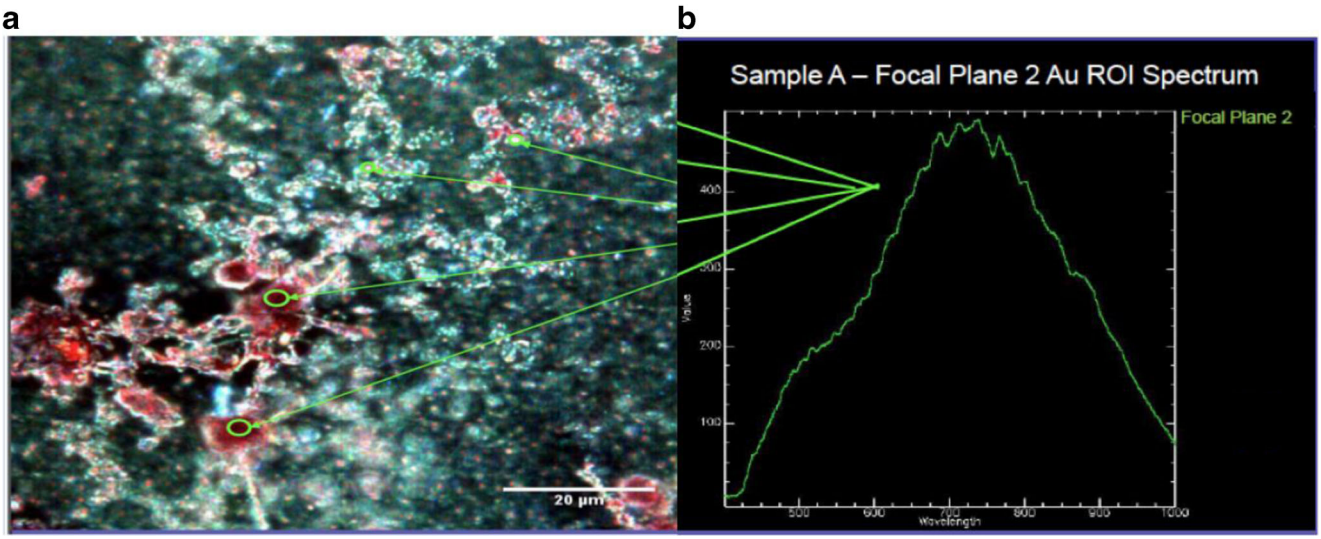

Fig. 7 Enhanced dark field hyperspectral imaging results of heated PVA. **a** Image. **b** Spectra

and, at the cross section of cut edges, to investigate the depth of particle embedding. Some samples were coated with 70 % gold and 30 % palladium to enhance the conductivity and facilitate detection of particle outlines. Raman spectroscopy was utilized to study the gold–polymer interactions. Raman maps were used in order to evaluate possible surface enhancement effects.

Lastly, a hyperspectral microscope was used, which has the capability to combine spectroscopy and imaging, focusing on individual particles or clusters for spectral analysis. This method enhances both the specificity and accuracy of the final spectral results, in addition to providing highly valuable images.

Results and Discussion

Structure and Morphology

X-ray diffraction measurements were performed on a heated PVA substrate with gold nanoparticles, in addition to a glass slide without any polymer with a deposit of AuNPs on its surface. The presence of the polymer results in a strong band at roughly 18 nm, whereas AuNPs and glass alone show no band. The Au film on the polymer substrate appears to be partially crystalline with a small crystal size and broader peaks.

The images shown in Fig. 4 reveal the presence of gold aggregates on the surface of heated PVA, SU-82, and PDMS films. The aggregates, which are distributed over the whole surface of the heated film (Fig. 5a, b), appear “folded.” The aggregation of gold nanoparticles that has been observed in the case of all polymer films studied in this work was submitted to repeated cycles of heating and cooling. Generally, the aggregates of gold nanoparticles show a de-clustering

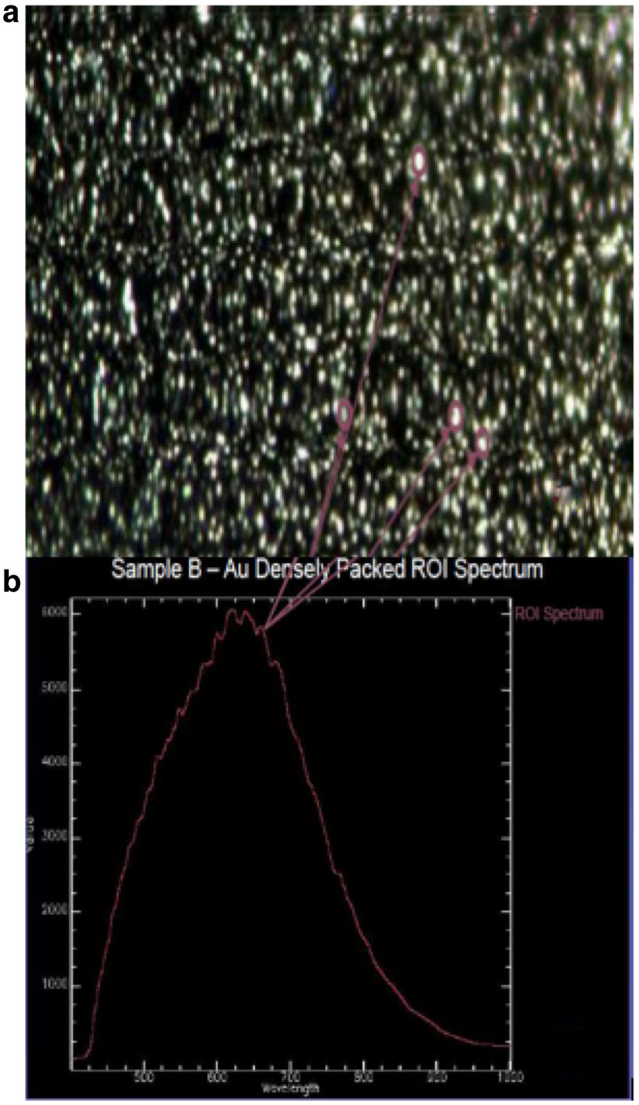

Fig. 8 Enhanced dark field hyperspectral imaging results of non-heated PVA. **a** Image. **b** Spectra

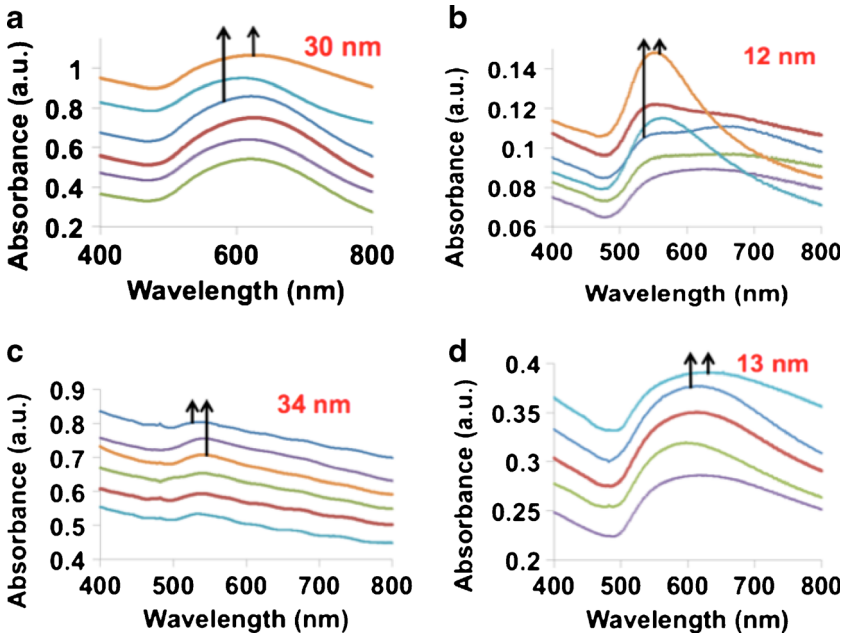

Fig. 9 Position of the Au plasmon band at different temperatures (80 °C (*dark blue*), 100 °C (*red*), 125 °C (*green*), 150 °C (*purple*), 175 °C (*light blue*), 200 °C (*orange*)) with the wavelength difference of the first and last bands for **a** PVA, **b** PDMS, **c** SU-82, and **d** PS

tendency when annealed at higher temperatures (around 500 °C), but in the case of the lower temperatures (200 °C) used in this work as well as because of the heating/cooling cycles, the aggregates remain stable. Figure 5c shows the highly porous structure of the PVA film. This particular morphology may be advantageous for the adsorption and stabilization of gold nanoparticles during the thermal convective deposition process. The SEM cross-section images corresponding to Au-PVA, Au-SU-82, and Au-PDMS nanocomposites are shown in Fig. 4 to discern the physical interface between gold and polymer. It can be seen that, before the samples are heated (Fig. 4a), the gold particles are evenly arranged across the top of the polymer, and no migration into the polymer is evident. In the images corresponding to the cross sections of the heated polymers (Fig. 4b, c), the gold nanoparticles have migrated (diffused) into the polymer bulk, to various degrees among different polymers. In Fig. 4b, which shows the heated PVA sample, it can be seen that a dozen or so particles have undergone penetration across a span of roughly 3 μm into the polymer film. In Fig. 4c, which shows a heated Au-SU-82 composite, the particles seem mostly gathered towards the top of the sample, but a few nanoparticles can be seen quite deep in the bulk. Similarly, in an experiment carried out by Putla, it was observed on a poly(-styrene) film bearing AuNPs that the nanoparticles embed into the polymer partially at the end of heating for 10 min at 45 °C [16].

The surface and cross section of the Au-PVA nanocomposites were also examined using AFM, as shown in Fig. 6. The images display an expected discrepancy in surface roughness between heated and non-heated samples. The heated PVA surface, shown in Fig. 6b, has, on average, 20 nm less roughness than a surface of PVA at room temperature, as shown in Fig. 6a. There is also a clear difference in the visual texture of the surface between both images, where the heated sample appears darker in general, with a fewer bright patches. The rightmost image, Fig. 6c, is a cross-sectional view of the heated PVA substrate, showing an aggregation of particles of some micrometers into the bulk of the film. The height indicated, which has a range of 200 nm, may correspond to the horizontal clustering of particles. This is in agreement with the hyperspectral images shown in Fig. 6.

In a related work by Karakouz et al. which involved AuNPs directly on a glass substrate without an intervening polymer film, it was found that the morphology of the glass substrate after annealing showed depressions in the glass similar in spacing to the AuNPs [18].

Employing a dark field hyperspectral microscope, the results of which are shown in Fig. 6, allows one to detect the substrate with clear and precise images of the particles on the surface of the polymer. Additionally, the spectral analysis may be done at specific regions of interest, enabling the measurement of individual

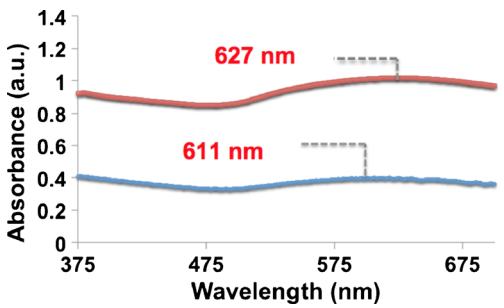

Fig. 10 Au LSPR band corresponding to incrementally-heated Au-PVA sample (*red*) and to the continuously heated sample (*blue*)

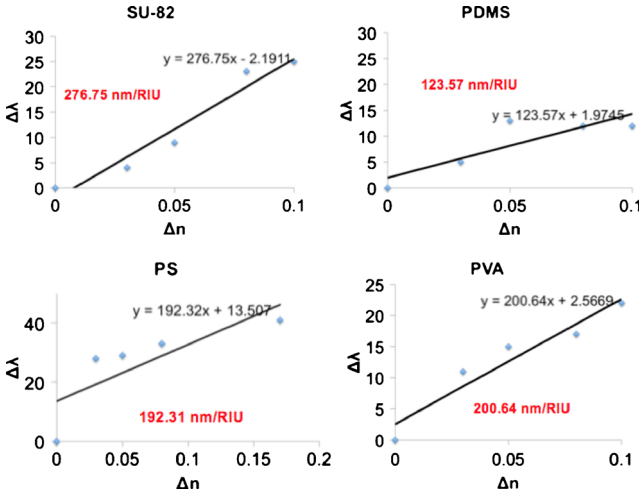

Fig. 11 Sensitivity of Au–polymer platforms measuring LSPR shifts in various solvents relative their refractive indices

particles and clusters, providing higher sensitivity than LSPR measurements. In Fig. 7, which shows particles inside a heated PVA polymer layer, the particles seem to have clustered to one area, compared to the image corresponding to the particles in the non-heated polymer. Their LSPR band averages to around 700 nm. In Fig. 8, which displays the nanoparticles at the surface of the non-heated polymer film, there is a more even distribution and very little aggregation is observed. Individual spectral measurements average to a lower value (roughly 650 nm) compared with the heated composite. The images corroborate the concept of particle clustering and penetration into the polymer film with heat, and the spectra confirm that when the particles have aggregated, they exhibit stronger scattering properties and produce a longer band wavelength as shown also by the UV–visible spectra of aggregated gold nanoparticles [17].

Spectral Properties

Figure 9 shows a series of LSPR bands corresponding to four surface nanocomposites with gold, throughout the gradation of heat treatments. These bands correspond to Au nanoparticles in the surface layer of the polymer films. The spectra show that, when the temperature is gradually increased, the bands appear to be shifted to longer wavelengths (redshifts). Karakouz has found that UV–vis spectra underwent a redshift in the SP band with heating [19]. Similarly, Putla has shown that when the sample temperature is increased to 45 °C, the LSPR band was redshifted by 4 nm [17].

The Au plasmon band corresponding to the Au-SU-82 nanocomposite showed a shift from 525 to 559 nm. The transition was mostly steady, with a general pattern of individual bands dipping slightly in the 500 nm region and then rising again some 50 nm thereafter. The Au plasmon band of the Au-PDMS nanocomposite shows a shift of 12 nm, rising from the 530-nm value, with the greatest discrepancy occurring at 175 °C. The thermal threshold is defined as the temperature at which the greatest difference between spectral properties is shown. It may indicate the period when the polymer state is most amenable to reconfiguration and physisorption of gold nanoparticles, which is determined by the surface energy forces around the particles. An interesting inverse relationship exists between the glass transition temperature values of the polymers and the magnitude of the shift. The polymers PVA and SU-82 show the greatest shifts and a transition temperature (Tg) of 85 and 50 °C, respectively, whereas PDMS and PS have Tg of 125 and 90 °C, respectively.

Figure 10 confirms the higher sensitivity of the Au-PVA nanocomposite, subjected to incremental heating (λ = 627 nm), compared to the sample heated directly to 200 °C (λ = 611 nm).

The resulting data is incorporated into a graph where the *y*-axis is the peak wavelength difference to water, and the *x*-axis is the refractive index difference to water. The slope of the trend line, measured in nanometer per refractive index units (nm/RIU), gives an indication of the sensitivity of these gold-bearing polymers. The sensitivity of the nanocomposite platform is shown in Fig. 11. In correlation with the magnitude of

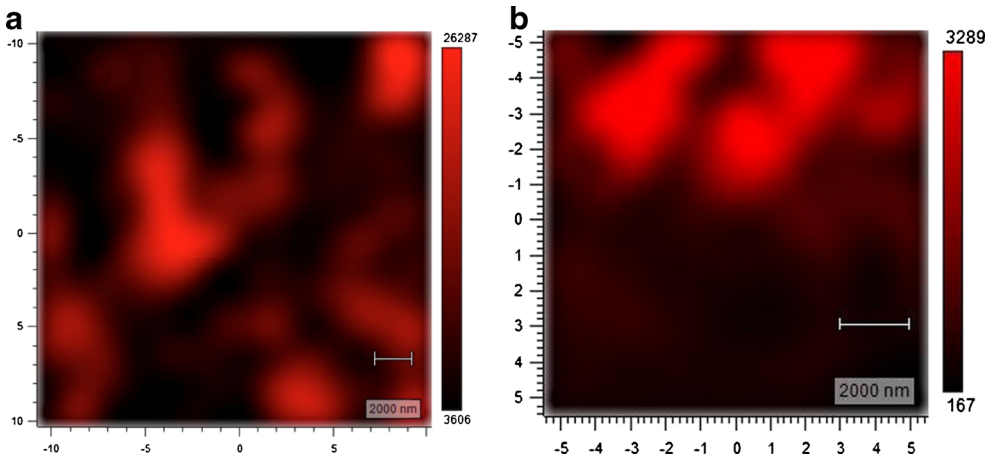

Fig. 12 Raman spectroscopy map (image created from compilation of separate Raman spectra) for the non-heated Au-PVA (10 μm × 10 μm) (**a**) and heated at 175 °C (20 μm × 20 μm) (**b**)

LSPR shifts, PVA and SU-82 display the greatest sensitivity, with 200.64 and 276.74 nm/RIU respectively, whereas PDMS and PMMA have lower values, with 123.57 and 129.41 nm/RIU, respectively. This could be attributed to particles clustering more prominently in some materials, thereby scattering light better and reacting strongly in response to increasing refractive indices.

Figure 12 depicts a Raman spectroscopy "map image" of Au-PVA nanocomposites that is achieved by compiling individual spectral intensities at one band, in this case at 1500 cm Raman shifts. This region is where the polymer exhibits a peak, and the gold material does not. The ratio of the two bands depends on the position of material on the map. A map image was performed for both heated and non-heated Au-PVA samples. In direct juxtaposition, a number of dissimilarities are apparent. There is an even dispersion of red and black (corresponding to gold) patches on the non-heated PVA. In contrast, the heated sample displays a concentration of red blotches on the top half of the measured area. This trend may result from an aggregation of particles across the surface of the polymer, indicating that, once heated, the polymer is more conducive to particle mobility and enables their convergence through the affinity of their surface energies. Another distinction between the images is the degree of intensity of the spectra. The scale bar at the right hand of the image of the heated sample is 3289, approximately eightfold smaller than the non-heated sample at 26284. This may be due to a smoothening of the polymer surface as result of the embedded gold nanoparticles in the polymer, which would diminish the protrusion of particles across the polymer surface and decrease spectra intensities. Karakouz et al. have found that annealing for 10 h at 600 °C leads to aggregation of closely spaced NPs, forming considerable clusters of particles [19].

In summary, both the morphological and the spectral studies are showing marked differences between the Au–polymer nanocomposites studied in this work. The differences originate in the structure of the surface layer of the polymer where the gold nanoparticles are hosted as well as in the specific thermal properties of the polymer, that is, their softening and glass transition temperatures, respectively. The position of the Au LSPR band in the nanocomposite, which is extremely sensitive to the dielectric environment, is the result of several concurrent phenomena, namely, softening of the polymer surface layer and partial or total embedding of gold nanoparticles, formation of gold aggregates having various sizes and shapes, and possible interactions between the gold particles or aggregates and the polymer chains. From this point of view, one can understand why the Au-PVA nanocomposite band shows an enhanced sensitivity after the heat treatment. Indeed, the polymer has a bulk glass transition temperature of 85 °C and the AFM and SEM images show some embedded particles into the surface layer and the presence of gold aggregates on the surface.

Conclusion

Gold–polymer surface nanocomposites have been prepared by depositing pre-synthesized gold colloids on the surface of polymer films, by using the thermal convection method. Subsequently, the films hosting the gold aggregates on their surface were heated incrementally at temperatures in the range of 80 to 200 °C and the morphology and spectral properties of the nanocomposite were investigated. The results pointed to the following conclusions: the incremental heating, alternating with short cooling periods, leads to the formations of small gold aggregates on the surface, together with a partial or total embedding of a part of the particles into the surface layer of the polymer. This configuration results in a large redshift of the Au LSPR band and, consequently, in an enhanced sensitivity of the nanocomposite platform. The results of this study will be helpful in selecting the most suitable materials for microfluidic sensing.

References

1. Barber DJ, Freestrone IC (1990) An investigation of the origin of the colour of the lycurgus cup by analytical transmission electron microscopy. Archaeometry 32:33–45
2. Neri A (1612) L'arte vetraria. Giunti, Firenze
3. Caseri WR (2014) In situ synthesis of polymer-embedded nanostructures. Nanocomposites: In situ Synthesis of Polymer-Embedded Nanostructures 1:45–47
4. Nicolais L, Carotenuto G (2014) Preparation and characterization of metal-polymer nanocomposites. Nanocomposites: In situ Synthesis of Polymer-Embedded Nanostructures 1:73–96
5. Katz E, Willner I (2004) Integrated nanoparticle-biomolecule hybrid systems: synthesis, properties, and applications. Angew Chem 43:6042–6108
6. Jain PK, Lee KS, El-Sayed IH, El-Sayed MA (2006) Calculated absorption and scattering properties of gold nanoparticles of different size, shape, and composition: applications in biological imaging and biomedicine. J Phys Chem 110:7238–7248
7. Huang X, El-Sayed IH, Qian W, El-Sayed MA (2006) Cancer cell imaging and photothermal therapy in the near-infrared region by using gold nanorods. J Am Chem Soc 128:2115–2120
8. Durr NJ, Larson T, Smith DK, Korger BA, Sokolov K, Ben-Yakar A (2007) Two-photon luminescence imaging of cancer cells using molecularly targeted gold nanorods. Nano letter 7:941–945
9. Nasir SM, Nur H (2008) Gold nanoparticles embedded on the surface of polyvinyl alcohol layer. Journal of Fundamental Sciences 4: 245–252
10. Liu FK, Hsieh SY, Ko FH, Chu TC (2003) Synthesis of golf/poly(methyl methacrylate) hybrid nanocomposites. Colloids and Surfaces 231:31–38
11. Loo C, Lowery A, Halas N, West J, Drezek R (2005) Immunotargeted nanoshells for integrated cancer imaging and therapy. Nano Lett 5:709–711
12. Uehara N (2010) Polymer-functionalized gold nanoparticles as versatile sensing materials. Anal Sci 26:1219–1228
13. Ramesh GV, Porel S, Radhakrishnan TP (2009) Polymer thin films embedded with in situ grown metal nanoparticles. Chem Soc Rev 38:2646–2656

14. Alsawafta M, Badilescu S, Paneri A, Truong VV,M, Packirisamy M (2011) Gold-poly(methyl methacrylate) nanocomposite films for plasmonic biosensing applications. Polymers 3:1833–1848
15. Porel S, Singh S, Harsha SS, Rao DN, Radhakrishnan TP (2005) Nanoparticle embedded polymer: in situ synthesis, free-standing films with highly monodisperse silver nanoparticles and optical limiting. Chem Mater 17:9–12
16. Putla RK (2010) Monitoring of glass transition at a polymer surface by localized surface plasmon resonance. Thesis Oklahoma State University
17. Pini V, Kosaka PM, Ruz JJ, Malvar O, Encinar M, Tamayo J, Calleja M (2016) Spatially multiplexed dark-field microspectrophotometry for nanoplasmonics. Nature Scientific Reports
18. Karakouz T, Maoz BM, Lando G, Vaskevich A, Rubinstein I (2011) Stabilization of gold nanoparticle films on glass by thermal embedding. Applied Material & Interfaces 3:978–987